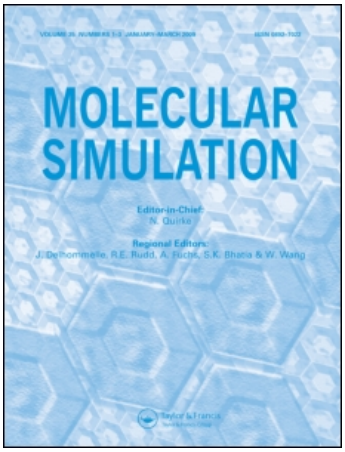

Molecular Simulation
Publication details, including instructions for authors and subscription information:
http://www.informaworld.com/smpp/title~content=t713644482

Applications of DL_POLY to modelling of mesoscopic particulate systems

J. A. Elliott[a]; M. Benedict[a]; M. Dutt[a]
[a] Department of Materials Science and Metallurgy, University of Cambridge, Cambridge, UK

To cite this Article Elliott, J. A. , Benedict, M. and Dutt, M.(2006) 'Applications of DL_POLY to modelling of mesoscopic particulate systems', Molecular Simulation, 32: 12, 1113 — 1121
To link to this Article: DOI: 10.1080/08927020600978846
URL: http://dx.doi.org/10.1080/08927020600978846

Molecular Simulation, Vol. 32, Nos. 12–13, 15 October–15 November 2006, 1113–1121

Taylor & Francis
Taylor & Francis Group

Applications of DL_POLY to modelling of mesoscopic particulate systems

J. A. ELLIOTT*, M. BENEDICT and M. DUTT

Department of Materials Science and Metallurgy, University of Cambridge, Cambridge CB2 3QZ, UK

(Received July 2006; in final form August 2006)

The molecular dynamics package DL_POLY has at its heart a number of versatile and efficient dynamics algorithms that can readily be adapted to extend the application of this code well beyond the time and length scales typically associated with atomistic simulations. In order to achieve this, it is necessary to substitute the appropriate interparticle potentials and forces in place of the default functional forms in DL_POLY, which are mainly suitable for molecular systems. To facilitate this, it may be required to incorporate additional factors, into the simulation, such as velocity-dependent dissipation effects (friction), rotational degrees of freedom and non-spherosymmetric forces. In this paper, we will discuss some of the practical details of implementing these changes to DL_POLY (version 2) together with applications of discrete particle dynamics methods, such as dissipative particle dynamics (DPD) and granular dynamics (GD) (also known as the discrete or distinct element method, DEM) to particle packing in composite systems and pharmaceutical powders. We also consider how well the approach of simulating particles of arbitrary shape using rigid assemblies of fused soft spheres (each individually interacting via pairwise continuous potentials) compares to true hard-body simulations of polygonal particles.

Keywords: DL_POLY; Granular dynamics; Discrete element method; Dissipative particle dynamics; Mesoscale simulation

1. Introduction

The classical molecular mechanics approach [1], which regards atomistic systems as being composed of discrete atomic particles interacting via a set of parameterised potential energy functions known as the "force field", is now widely used in the field materials science [2]. As a result of its popularity, there are now many freely available software packages, as well as commercial codes, which can carry out energy minimisation or exploration of phase space via molecular dynamics using the atomistic force fields. One such package, available under license from Daresbury Laboratory, is DL_POLY [3]. We shall not attempt to describe the full functionality of the various versions of DL_POLY in detail here, but suffice to say that the package contains a number of efficient parallelised algorithms for carrying out molecular dynamics of free or partially constrained atomic particles and rigid bodies in various thermodynamic ensembles. It has also been well validated over a wide range of applications by a worldwide community of scientists and engineers. Perhaps the most important benefit is the availability of source code for the package, which enables substantial changes to the types of systems that can be simulated. It is our intention in this paper to describe the modifications made to DL_POLY in our research group in order to study mesoscopic particulate systems, in which the particles are many orders of magnitude larger than atoms, but where the fundamental classical equations of motion to be solved remain essentially the same (i.e. those based on Newton's second law, which can be formulated via an extended Lagrangian). Using our customised versions of DL_POLY, we have been able to study phenomena as diverse as packing of filler particles in polymer composites [4], compaction of pharmaceutical powders [5] and electrical percolation in carbon nanotube (CNT) networks [6]. Of course, our work in this area is not in isolation, and many other research groups have investigated such types of systems using methods variously described as discrete or distinct element methods (DEM) [7–11], granular dynamics (GD) [12–14], Brownian dynamics (BD) [15] and dissipative particle dynamics (DPD) [16–19]. It should be noted that DEM and GD are virtually indistinguishable from a computational perspective, but

*Corresponding author. Email: jae1001@cam.ac.uk

Molecular Simulation
ISSN 0892-7022 print/ISSN 1029-0435 online © 2006 Taylor & Francis
http://www.tandf.co.uk/journals
DOI: 10.1080/08927020600978846

the former term is commonly used by engineers in UK and USA and physicists in USA, whereas the latter term is most commonly used by physicists in the UK. The wider applications of mesoscale particulate methods extend to computational fluid dynamics and thermal or mass transport problems, where robust alternatives to finite element analysis can be formulated based on a particle-based schemes [20].

The most significant difference between atomistic and mesoscopic particulate systems is of course the particle size, with atoms and molecules lying in the range of 0.1–1 nm, and colloidal or granular particles in the range of 0.11–100 μm. Thus, while the former are dominated by interatomic bonding and electrostatic forces, the latter can also be strongly influenced by excluded volume and geometric packing considerations. Furthermore, while interatomic interactions tend to be on the whole spherically symmetric, often defined using simple pair potentials, larger particles can have a complex shape-dependence to their behaviour. Although shape-dependent intermolecular interactions do exist, such as the Gay-Berne potential [21] for modelling rod-like or discotic liquid crystals, they are usually based on perturbations to spheroidal particles. For mesoscopic particles with a high degree of angularity, such a perturbative approach may not be sufficient to capture the essential physics of the particle behaviour, including the phase behaviour (where differences in particle shape can lead to segregation). In Section 2.3, we examine the extent to which angular particles can be modelled by the use of assemblies of fused soft spheres in DL_POLY by comparison with a full hard-body impulsive molecular dynamics calculation using one of our own codes MD-ARG.

At the mesoscopic scale, new types of interactions can emerge, such as contact friction or other dissipative forces, which are a result of the averaged ensemble behaviour of microscopic degrees of freedom. The incorporation of these new types of interactions couples together the translational and rotational degrees of freedom of the mesoscopic particles, and can lead to a loss of thermodynamic behaviour (e.g. in a flowing sandpile which comes to rest under the influence of internal friction) if the dissipative forces are not balanced by a commensurate energy input via a Langevin force (i.e. thermal energy) or some other external source (e.g. mechanical agitation). In Section 2.2 we discuss the non-thermodynamic effects of contact frictional forces in GD simulations, whereas in Section 2.1 we focus on thermodynamic behaviour where the dissipation is counterbalanced by injection of thermal energy.

We begin by outlining the modifications required to the standard DL_POLY package (for simplicity, all references are to version 2.14) and then summarise some of our published results obtained with the modified programs. We will assume that that reader is familiar with the structure of the DL_POLY code, as set out in the DL_POLY reference manual [3].

2. Computational methodology

2.1. Dissipative particle dynamics with DL_POLY

DPD is a mesoscale method for dynamical simulations of soft colloidal particles, which are often supposed to be coarse-grained models for clusters of atomic particles. First proposed by Hoogerbrugge and Koelmann [22,23], and then subsequently refined, by Español [24], it is based on coarse-graining the motion of fluid-like particles surrounding the DPD particles into two pairwise-acting fictitious forces consisting of a dissipative and a random (Langevin) term, respectively. The functional forms of these so-called DPD forces must be carefully chosen to obey a fluctuation–dissipation theorem which produces an equilibrium temperature within the simulation. The fact that all forces are pairwise-acting guarantees Galilean invariance, and the resulting mass and momentum transport in the simulation can be shown to result in macroscopic Navier–Stokes behaviour in the hydrodynamic limit [24]. Since the original formulation had some problems with physical interpretation of the DPD parameters, and had a restricted equation of state, it has more recently been reformulated within a more general thermodynamic framework [25,26]. However, the implementation described in this paper is similar to that used by Groot and Warren [17], which is adequate for the purposes described herein, although similar principles could easily be applied to the implementation of the revised formulation.

In order to implement DPD within the DL_POLY code, the dissipative and random forces must be included. The functional forms are given by Groot and Warren [17], and since these are short-ranged, it is straightforward to include them in the existing subroutine `srfce.f`, which is conventionally used to generate short-ranged molecular forces. One important point to note is that dissipative force depends on the relative particle velocities, which must be passed through the main program into `srfce.f`. Furthermore, the random (Langevin) force requires a source of normally distributed random numbers with zero mean and unit variance. Since each pair of dissipative particle contacts requires one random number per time step, then a very large quantity of uncorrelated normally distributed numbers are required. The conventional method within DL_POLY of summing many independent uniformly random variables to yield a normally distributed variable (via the Central Limit Theorem), such as employed when generating the initial velocity distribution, is much too time-consuming to be employed for the evaluating the random force. For this reason, a supplementary routine was incorporated for generating normally distributed random variables via the Box-Muller method. Nevertheless, profiling tools indicated that a non-negligible fraction of total CPU time is still spent evaluating random numbers for use in the DPD force routine.

Since the DPD forces automatically generate configurations in the NVT ensemble, there is a need to modify existing integration routines to ensure that there is no attempt to rescale particle velocities. This entailed total removal of the thermostat and decoupling of the translational velocities from barostat variables in the `nvt_h1.f` and `npt_h1.f` routines for single particles, and `nvtq_h1.f` and `nptq_h1.f` routines for rigid bodies. It was found that the action of the barostat on the particle positions alone (i.e. by the warping of cell volume) was sufficient to achieve a constant pressure, constant temperature ensemble. The effect of these modifications is to remove all fictitious forces acting in the system, save for those introduced in `srfce.f` for the DPD dissipative and random terms. This is a necessary step in order to preserve the hydrodynamic behaviour of the mesoscopic particles, since all remaining forces in the simulation (including the energy-conserving terms) are pairwise-acting. The effects of hydrodynamic interactions on configurations of particles generated using DPD are described in Section 3.3

2.2. Granular dynamics with DL_POLY

GD is a numerical method for simulating the dynamics of semi-rigid macroscopic frictional particles with sizes ranging from tens of metres to micrometres, such as pharmaceutical powders, talcs, cement, sand and rocks. In the absence of an interstitial medium, these particles interact with one another via short-range contact mechanical forces [27,28], which include both elastic and viscoelastic components, along with macroscopic surface friction. The nature of the interactions coupled with the size of the particles (relative to atomic and molecular systems) are such that the dynamics of these systems is rapidly quenched due to the dissipative interactions, unless there is energy input in the form of mechanical excitation. Cundall and Strack [29] developed GD, or DEM, to study geophysical systems using simple linear damped spring force models to represent the interactions. Since then the numerical representation of the pairwise particle interactions have evolved to incorporate force-displacement (linear spring, Hertzian) and force-displacement-velocity (spring-dashpot, Hertz-Mindlin, Hertz–Kuwabara–Kono (HKK)) models which account for experimentally measured material properties such as the Young's modulus, Poisson's ratio and surface friction [30,31]. Macroscopic surface friction between particle surfaces is accounted for via the use of Coulomb's yield criteria [32,33]. The nature of the contact forces, which act parallel and perpendicular to the vector connecting the centres of mass of the interacting particles, require a coupling between translational and rotational degrees of freedom, as the effective tangential force applies a torque on the particle. In this paper, we focus on systems pertaining to the shorter length scales for granular systems, in the range of 10–100 μm and have used DL_POLY to develop a mesoscopic GD simulation to study the statics and dynamics of pharmaceutical powders [5].

The implementation of GD into the DL_POLY framework required incorporation of the contact forces, coupling of the rotational and translational degrees of freedom, changes to the neighbour list algorithm and the integration routine `nveq_1.f`. A new subroutine `contact_forces_hkk.f` was developed to include the HKK and spring-dashpot force models along the normal and tangential direction, together with the Coulomb's yield criteria using the functional forms provided in Dutt *et al.* [5]. These forces are calculated for only those particle pairs which are overlapping. In addition, we introduced coupling between the rotational and translational degrees of freedom by including a pairwise tangential force that produces a torque acting on contacting particles about the line connecting the centre of each particle to the point of contact. As a consequence, each particle can particle can acquire an angular velocity about its centre of mass. Due to nature of the interparticle interactions, we had to ensure that the neigbour list computations could account for current and imminent neighbours of a given particle. We modified `parlink.f` such that each link cell dimension was slightly larger than the largest interparticle contact separations with zero overlap by a distance known as r_{skin}, which determines the frequency of computation of the neighbour list. Also, the criteria used to determine membership of a given neighbour list depends on the comparison between the interparticle distances with the sum of the centres of mass separation at contact (but with zero deformation) and r_{skin}. The time integration subroutine `nveq_1.f` was modified to remove the constant energy implementation and update all the translational and rotational degrees of freedom. The effect of the above modifications on the system dynamics is illustrated in Section 3.1

2.3. Dynamics of angular particles with DL_POLY

In an effort to better understand how complex phenomena such as flow and mixing depend on particle shape, and also to provide an exact reference system for extension through perturbation theory to real granular systems, standard molecular dynamics simulations were used to investigate the steady state phase behaviour of systems composed of several 1000 angular particles in microcanonical (NVE) and canonical (NVT) ensembles. To further investigate the need to simulate the precise angular shape of particles accurately, two different types of simulations were conducted. In the first series, DL_POLY was used to simulate collections of particles composed of dense, rigidly-bound spheres interacting via a short-range, purely repulsive potential defined between pairs of spheres. The arrangement of these spheres within each particle was designed to approximate the shape of a cube, although in principle any shape could be so modelled. This approach to modelling non-spherical particles, sometimes known as the "blackberry" model, has also been used by other

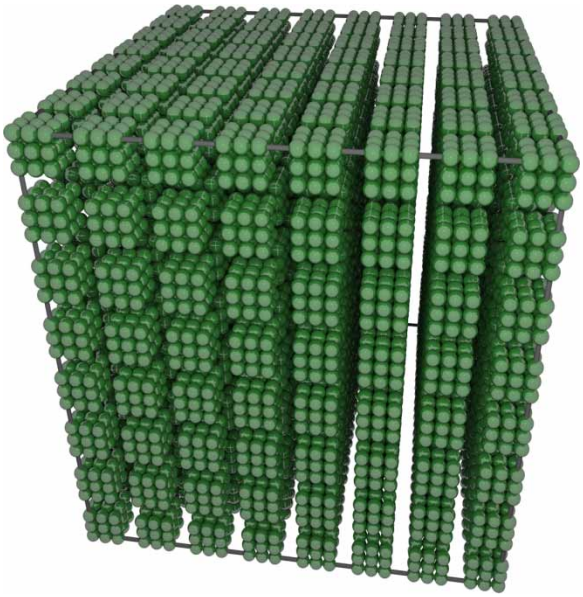

Figure 1. Simulation cell showing periodic lattice of 512 cuboid particles made from subdividing particles into spheres at $N = 3$ level.

researchers, see e.g. [34,35], but we are not aware of any systematic studies of the accuracy of such an approximation. In this paper, we investigate the sensitivity of the static and dynamical properties of the bulk system on the accurate representation of particle shape. The volume, mass and moments of inertia of the particles were fixed at constant values, and the size of the component spheres was decreased allowing a larger number of spheres to represent the shape. In a second series of simulations, used as a comparison for the limiting case of the previous simulations, full hard body calculations for a mixture of cubes were performed using our own impulsive molecular dynamics code MD-ARG.

Calculating the exact time to collision between two arbitrarily shaped objects is a computationally expensive process. When a large collection of N distinct particles is considered, this becomes at worst N^2, or at best $N \log N$, times more computationally expensive. When N exceeds several 100, this process can quickly scale beyond the computational resources currently available. One method to avoid these expensive collision time calculations is to approximate the shape desired with a rigidly bound collection of spheres. The collision time between two spheres is a simple quadratic equation related to the spheres' velocities and radii, and can be calculated many millions of times per second on modern computers. Provided the number of spheres needed to approximate the arbitrarily-shaped body does not become too large, it is possible to greatly accelerate the calculations and increase the system sizes it is possible to study.

However, a key assumption made in adopting the fused sphere approach is that a relatively small number of component spheres will provide a reasonable approximation of the excluded volume behaviour for the types of rigid bodies that make up colloidal and granular systems. To examine whether this assumption is valid, a series of computational experiments have been conducted using the rigid body algorithm of the DL_POLY. In an effort to approximate the excluded volume behaviour of a cubic rigid body we have chosen to represent the cube with a variable number of spheres. In this case, a cubic lattice, centred at the middle of the rigid cube, is subdivided into N divisions per linear dimension. Next, each of the lattice points is populated with a sphere whose radius is a function of the desired total excluded volume of parent cuboid particle. To accurately model the excluded volume effects of the cube it is important to carefully choose the volume of each particle in the simulation. The cuboids illustrated in figure 1 make it apparent that the excluded volume of the cuboid is a function of the number of spheres used to approximate the cube. The excluded volume of the cuboid is given by:

$$V_{\text{cuboid}} = A_c \cdot r_c^3 \tag{1}$$

where the factor in front of the cubic "radius" or half-width is given by:

$$A_c = [2(N-1)]^3 + \frac{4\pi}{3}[3N^2 - 3N + 1] \tag{2}$$

Setting the volume of the cube equal to that of a sphere allows us to define the radius of each component sphere on the lattice relative to the radius of the true sphere as:

$$r_{\text{cube}} = 0.483 \cdot r_{\text{sphere}} \tag{3}$$

for $N = 2$. Figure 2 depicts increasing levels of subdivision, stating at a total of eight spheres approximating a cube ($N = 2$), all the way up to 125 spheres approximating a cube ($N = 5$). As $N \rightarrow \infty$, it is reasonable to assume that the cuboid should reproduce exactly the behaviour of the true polyhedral cube.

The interactions between particles in a colloidal or granular system are dominated by the excluded volume, short-range repulsive behaviour of the particles. It has

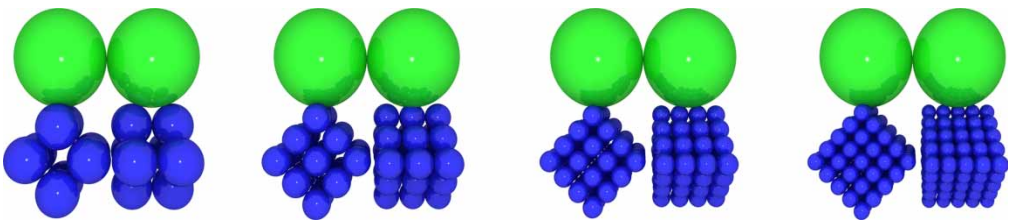

Figure 2. Cuboid particles approximated by increasingly fine-grained spherical subdivision, from $N = 2$ (left) to $N = 5$ (right).

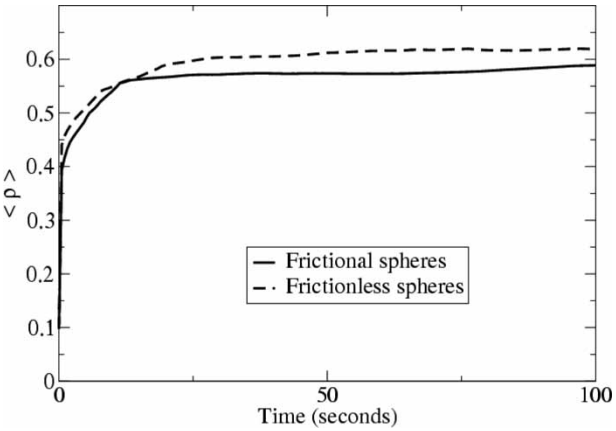

Figure 3. Time evolution of packing fraction for a 1000 particle system, with and without substrate friction.

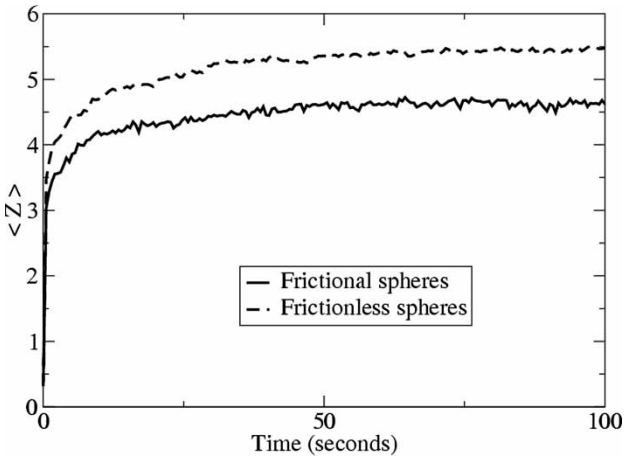

Figure 4. Time evolution of average coordination number $\langle Z \rangle$ for a 1000 particle system, with and without substrate friction.

been shown [36] that an inverse power potential such as:

$$U(r) = \varepsilon\left(\frac{\sigma}{r}\right)^n \tag{4}$$

can be an accurate model for interparticle interaction in colloidal and granular systems. Of particular interest is that when the hardness parameter, i.e. the exponent n, tends to infinity, the hard sphere model is recovered exactly. However, molecular dynamics algorithms will face numerical accuracy challenges if n becomes too large, so in order to agree with the experimental results for real colloidal systems, the exponent was given the fixed value of $n = 50$ by Bryant [37]. When used to calculate the pressure for a reference hard sphere system, this value for the exponent in the inverse power potential generated results to within 2–3% of literature values for the hard sphere system at the same number density. This indicates that this system should provide a reasonable point of comparison with a full rigid body calculation for the hard sphere and cube mixture.

In our case, the only modification required to DL_POLY to carry out simulations of angular particles was to add a purely repulsive $1/r^n$ type potential to the routine `srfce.f`. For the simulations presented in Section 3.2, the repulsive exponent was set to $n = 25$. Although it would have been desirable to set the exponent as high as possible to more closely simulate a hard particle system, this would have required lowering the integration time step to unacceptably low values in order to maintain numerical stability. Individual runs consisted of 512 spherically-subdivided cubes, which lead to a different number of spheres at each subdivision level. The increase in computational burden is significant, since the number of spheres that must be simulated grows with the cube of the subdivision level, making levels beyond $N = 5$ (i.e. 64,000 spheres in total) cumbersome in terms of memory usage and storage space. In Section 3.2, we investigate the level of subdivision that is required to reproduce the correct static and dynamic properties of a system of hard polygonal cubes.

3. Results

3.1. Granular dynamics of frictional spherical particles

Simulations were run to examine the packing of particles under gravity using monodisperse spherical particles, both with and without friction. A system of a 1000 particles was initialised in a dilute state, a low packing fraction of around 0.03, with none of the particles in contact. We introduced a substrate consisting of fused arrays of spheres [38] onto which the particles were allowed to settle under gravity. As the particles settle, we monitored the time evolution of the packing fraction and the average coordination number. As surface friction quickly dissipates the relative motion at the particle contacts, we would expect the packing fraction ρ and coordination number Z for frictional particles to be lower than that for frictionless particles. In figures 3 and 4, we found that both ρ and $\langle Z \rangle$ were indeed consistently lower throughout the simulation for the frictionless particles.

We also studied the effect of varying the fraction of softer (lower Young's modulus) to stiffer (higher Young's modulus) particles. In this case, the system of particles was bounded between two fixed substrates lying normal to the direction of gravity. We allowed the particles to initially settle under gravity onto a substrate for a given interval of time, followed by constant strain compaction applied, via the upper substrate, again for a fixed interval of time. We considered two samples with 1800 monodisperse spherical particles each. Sample S1 was made up of particles with the values of Young's modulus and Poisson's ratio of 3 GPa and 0.3, respectively. Sample S2 was made up of 900 particles having values of Young's modulus and Poisson's ratio of 3 GPa and 0.3, respectively, and the remaining 900 particles with values of Young's modulus and Poisson's ratio of 9 GPa and 0.3, respectively. We would expect that,

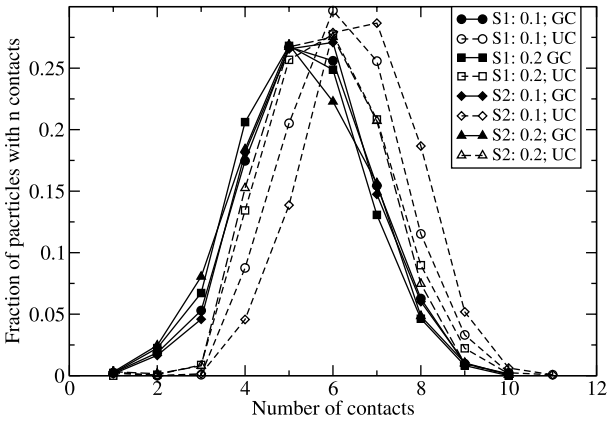

Figure 5. Distribution of contacts after particles were settled under gravity (GC), and after completion of the uniaxial compaction phase (UC). The two numbers in the legend represent the values of the coefficients of kinetic and static friction.

due to the larger degree of deformation of the softer particles as opposed to the harder particles, sample S1 would demonstrate higher average values of ρ and $\langle Z \rangle$. We found that for a given value of surface friction (represented by kinetic and static friction [5]), the distribution of contacts for S1, in comparison to S2, favoured a larger number of contacts both after the particles settled under gravity and also after completion of uniaxial compaction, as shown in figure 5. Similar trends were found for higher values of surface friction.

3.2. Smooth aspherical granular particles

Simulation runs for the spherically subdivided cuboids, as described in Section 2.3, were carried out using DL_POLY in the NVT ensemble using a Berendsen thermostat with a relaxation time of 5 ps. The run lengths were approximately 500 ps, using a timestep of 0.001 ps. The results were compared against an equivalent system of hard, polygonal cubes simulated using our own impulsive dynamics code MD-ARG.

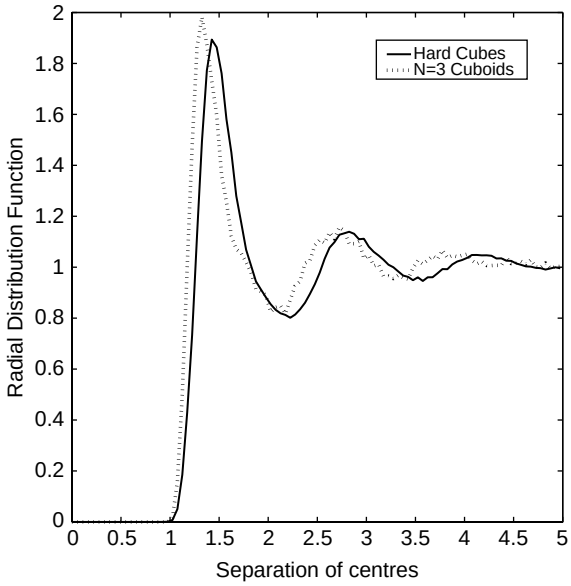

Figure 6. RDF for the hard polygonal cube system (solid line) and $N = 3$ spherically subdivided cuboids (dotted line), with x-axis normalised to the cube edge length.

Figure 6 shows the radial distribution function (RDF) for the hard cubes compared to that of the $N = 3$ subdivided cuboids. The x-axis gives the separation of centres of mass of the particles in units of the cube edge. Note that because the minimum separation distance between any two cubes is a continuous function of the relative orientations, the hard cube RDF has no sharp discontinuity, as is characteristic of the hard sphere RDF. The shape of the two curves is quite similar, indicating that the thermodynamic states of the two systems would also be similar, however there are some subtle differences that merit further discussion. In particular, the soft repulsive potential used to model the subdivided cuboids allows the particles to remain slightly closer to one another than in the hard cube system, as can be seen by the general shift to the left of the subdivided cuboid curve in figure 6. While the height of the second and third peaks appear quite similar between the two systems, the height of the first peak is somewhat higher in the subdivided cuboid system, and much of the thermodynamics, in particular the internal pressure, is related to this peak.

The self diffusion coefficient of the cubes (or cuboid centres-of-mass) was calculated from the simulation results using the Einstein relation. These data were used to compute the relative mobility of the cuboids, defined as the ratio of the spherically subdivided cuboid self diffusion coefficient to the self diffusion coefficient for the hard cubes. Figure 7 shows the relative mobility of the cuboids as a function of the subdivision level N. It is apparent that it is a rapidly converging function. In fact, by the fourth subdivision level, $N = 4$, rather lengthy simulation runs are required to discern any difference from the behaviour predicted by the hard cubes calculation. Even for the lowest level of subdivision, the agreement is reasonable.

3.3. Dissipative particle dynamics of spheres, cubes and rods

The DPD code described in Section 2.1 was combined with the method for anisotropic particle shape description by spherical subdivision of space described in Section 2.3 in order to carry out the simulation of a range of different mesoscopic particles suspended in a pseudo-fluid medium through which hydrodynamic forces may propagate. These forces are believed to be important in achieving equilibrium in ordered mesophases of complex systems [39–41]. Examples of the types of particles that can be modelled as shown in figure 8, and elsewhere we describe in the detail the investigation of binary mixtures of spheres of different sizes and cube-sphere mixtures with varying proportions of the components [4]. The conclusions from this work were that the results for soft repulsive sphere mixtures correspond very well to the predictions of

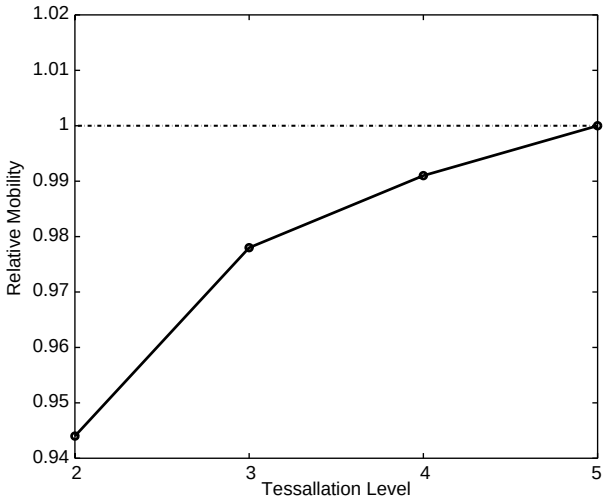

Figure 7. Relative mobility of centres of mass of cuboid particles to that of the polygonal cube mobility as a function of spherical subdivision level.

analytical equations of state in regions where an equivalence can be made to a hard sphere reference system. For systems of pure cuboids, a translationally disordered phase with cubatic orientational order was found above a particular critical pressure. In mixtures of spheres and cuboids, an entropically-driven demixing transition was observed. Although all of these results could have been obtained in principle using standard molecular dynamics, the attraction of using the DPD thermostat method is that hydrodynamic effects are preserved on the local scale, a fact which has also been noted by other authors [19].

More recently, we have focused attention on structure of fibre networks, where each fibre is modelled as a rigid assembly of spheres [6], as illustrated in figure 8 middle. Such networks can provide a good description of the onset of electrical percolation in CNT-polymer composites, in which the polymer matrix is considered to be a perfect insulator and the fibres (CNTs) are perfect conductors. The onset of electrical percolation is a function of both the loading fraction and orientational order of the fibre network. Figure 9 shows an example of a fibre network of 1125 fibres with occupied volume fraction 0.05 and aspect ratio $L/D = 10$, generated initially with perfect nematic order, figure 9(a), and after equilibration with DPD at 298 K in figure 9(b). The equilibrated network has isotropic orientational order, and the rate of relaxation is greatly enhanced by the use of DPD force interactions. Since the DPD method can also be applied to non-equilibrium situations, it is straightforward to examine the influence of external fields, such as electrical and shear fields, on fibre alignment (and hence electrical percolation behaviour). Further details of the network analysis are given elsewhere [6], but the principal conclusions are that isotropically oriented networks remain electrically percolating to much lower volume fractions than orientationally ordered networks, and that the sensitivity to orientational order becomes extreme in the case of higher aspect ratio fibres. The results obtained by DPD simulations correspond well to analytical theory for purely repulsive fibres, but the model has the capability to simulate the affects of fibre aggregation, and further work is currently in progress.

4. Summary and conclusions

In this paper, we have examined the dynamics of a number of different mesoscale systems, some of which are based on thermodynamic methods (e.g. DPD and standard microcanonical molecular dynamics) and others of which are non-thermodynamic (e.g. GD with viscoelastic force contact models). We have shown that with inclusion of appropriate contact force models it is possible to study the effects of frictional forces and single-particle mechanical properties of the packing structure of granular systems consisting of spherical particles. For aspherical particles, a spherical subdivision method is presented as a convenient means of mapping standard pair potentials onto systems containing objects of more complex shape. For the case of purely repulsive cuboids, both static and dynamical properties of the system agree very well with full hard body polygonal cubes for modest levels of spherical subdivision. Using this subdivision method, we have studied the DPD of a range of different particles systems, in particular the evolution of orientational order in fibre networks as models for electrically conducting nano-composites. We anticipate that the methods described in

Figure 8. Examples of particulate systems which can be modelled using a combination of DPD thermostat and the spherical subdivision description of particle shape, from left to right: binary sphere mixture, fibres, and cuboids.

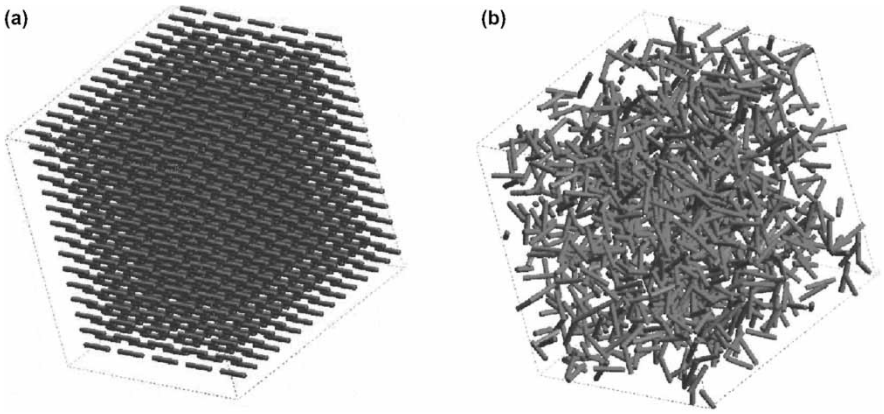

Figure 9. Fibre networks generated from 1125 fibres with aspect ratio $L/D = 10$ and volume fraction 0.05, using a spherical subdivision representation: (a) initial nematic array, and (b) isotropic array after relaxation via DPD.

this paper may be of use to other researchers looking to use mesoscale particle methods with DL_POLY.

Acknowledgements

The authors are grateful to a number of funding bodies for financial support for the various parts of this work, including the Engineering and Physical Sciences Research Council (EPSRC), Pfizer Inc., the US Air Force (under contract S-709-009-014/D) and the US Army European Research Office (under contract N6255-020C9014). The use of data from the PhD thesis of Sameer S. Rahatekar (figure 9) is acknowledged.

References

[1] A.R. Leach. *Molecular Modelling: Principles and Applications*, 2nd ed. Prentice-Hall, New Jersey (2001).
[2] S. Yip (Ed.). *Handbook of Materials Modeling*, Springer, New York (2005).
[3] T.R. Forester, W. Smith. *DL_POLY molecular dynamics code*, CCP5 of the EPSRC (1995).
[4] J.A. Elliott, A.H. Windle. A dissipative particle dynamics method for modelling the geometrical packing of filler particles in polymer composites. *J. Chem. Phys.*, **113**, 10367 (2000).
[5] M. Dutt, B.C. Hancock, A.C. Bentham, J.A. Elliott. An implementation of granular dynamics for simulating frictional elastic particles based on the DL_POLY code. *Comput. Phys. Commun.*, **166**, 26 (2005).
[6] S.S. Rahatekar, M. Hamm, M.S.P. Shaffer, J.A. Elliott. Mesoscale modelling of electrical percolation in fibre-filled systems. *J. Chem. Phys.*, **123**, 134702 (2005).
[7] Y. Tsuji, T. Kawaguchi, T. Tanaka. Discrete particle simulation of 2-dimensional fluidized-bed. *Powder Technol.*, **77**, 79 (1993).
[8] R.W. Lewis, D.T. Gethin, X.S.S. Yang, R.C. Rowe. A combined finite-discrete element method for simulating pharmaceutical powder tableting. *Int. J. Numer. Methods Eng.*, **62**, 853 (2005).
[9] A. Hassanpour, M. Ghadiri. Distinct element analysis and experimental evaluation of the Heckel analysis of bulk powder compression. *Powder Technol.*, **141**, 251 (2004).
[10] C. Thornton, K.K. Yin, M.J. Adams. Numerical simulation of the impact fracture and fragmentation of agglomerates. *J. Phys. D: Appl. Phys.*, **29**, 424 (1996).
[11] C. Thornton, M.T. Ciomocos, M.J. Adams. Numerical simulations of agglomerate impact breakage. *Powder Technol.*, **105**, 74 (1999).
[12] J.A.C. Gallas, H.J. Herrmann, T. Poschel, S. Sokolowski. Molecular dynamics simulation of size segregation in three dimensions. *J. Stat. Phys.*, **82**, 443 (1996).
[13] H.J. Herrmann, S. Luding. Modeling granular media on the computer. *Continuum Mech. Thermodyn.*, **10**, 189 (1998).
[14] M. Moakher, T. Shinbrot, F.J. Muzzio. Experimentally validated computations of flow, mixing and segregation of non-cohesive grains in 3D tumbling blenders. *Powder Technol.*, **109**, 58 (2000).
[15] R.C. Ball, J.R. Melrose. A simulation technique for many spheres in quasi-static motion under frame-invariant pair drag and Brownian forces. *Physica A*, **247**, 444 (1997).
[16] P.V. Coveney, P. Español. Dissipative particle dynamics for interacting multicomponent systems. *J. Phys. A: Math. Gen.*, **30**, 779 (1997).
[17] R.D. Groot, P.B. Warren. Dissipative particle dynamics: bridging the gap between atomistic and mesoscopic simulation. *J. Chem. Phys.*, **107**, 4423 (1997).
[18] S. Jury, P. Bladon, M.E. Cates, S. Krishna, M. Hagen, N. Ruddock, P. Warren. Simulation of amphiphilic mesophases using dissipative particle dynamics. *Phys. Chem. Chem. Phys.*, **1**, 2051 (1999).
[19] T. Soddemann, B. Dunweg, K. Kremer. Dissipative particle dynamics: A useful thermostat for equilibrium and nonequilibrium molecular dynamics simulations. *Phys. Rev. E.*, **68**, 046702 (2003).
[20] R.W. Hockney, J.W. Eastwood. *Computer Simulation Using Particles*, McGraw-Hill, New York (1981).
[21] J.G. Gay, B.J. Berne. Modification of the overlap potential to mimic a linear site–site potential. *J. Chem. Phys.*, **74**, 3316 (1981).
[22] P.J. Hoogerbrugge, J.M.V.A. Koelman. Simulating microscopic hydrodynamic phenomena with dissipative particle dynamics. *Europhys. Lett.*, **19**, 155 (1992).
[23] J.M.V.A. Koelman, P.J. Hoogerbrugge. Dynamic simulations of hard-sphere suspensions under steady shear. *Europhys. Lett.*, **21**, 363 (1993).
[24] P. Español. Hydrodynamics from dissipative particle dynamics. *Phys. Rev. E.*, **52**, 1734 (1995).
[25] P. Español, M. Serrano, H.C. Öttinger. Thermodynamically admissible form for discrete hydrodynamics. *Phys. Rev. Lett.*, **83**, 4542 (1999).
[26] P. Español, M. Revenga. Smoothed dissipative particle dynamics. *Phys. Rev. E.*, **67**, 026705 (2003).
[27] H.M. Jaeger, S.R. Nagel, R.P. Behringer. Granular solids, liquids, and gases. *Rev. Mod. Phys.*, **68**, 1259 (1996).
[28] K.L. Johnson. *Contact Mechanics*, Cambridge University Press, UK (2001).
[29] P.A. Cundall, O.D.L. Strack. Discrete numerical-model for granular assemblies. *Géotechnique*, **29**, 47 (1979).
[30] J. Schäfer, S. Dippel, D.E. Wolf. Force schemes in simulations of granular materials. *J. Phys. I France*, **6**, 5 (1996).
[31] E.M. Lifshitz, L.D. Landau. *Theory of Elasticity*, Vol. 7, 3rd ed. Butterworth-Heinemann, Oxford (1986).
[32] C. Coulomb. *Memoir De Mathematique Et De Physique*, Vol. 7, p. 343, Academie des Sciences, L' Imprimerie Royale, Paris (1773).
[33] J.A. Åström, H.J. Herrmann, J. Timonen. Granular packings and fault zones. *Phys. Rev. Lett.*, **84**, 638 (2000).

[34] K.E. Evans, M.D. Ferrar. The packing of thick fibres. *J. Phys. D: Appl. Phys.*, **22**, 354 (1989).
[35] F.X. Sanchez-Castillo, J. Anwar, D.M. Heyes. Molecular dynamics simulations of granular compaction: The single granule case. *J. Chem. Phys.*, **118**, 4636 (2003).
[36] D. Heyes, J. Powles. Thermodynamic, mechanical and transport properties of fluids with steeply repulsive potentials. *Mol. Phys.*, **95**, 259 (1998).
[37] G. Bryant, S.R. Williams, L. Qian, I.K. Snook, E. Perez, F. Pincet. How hard is a colloidal "hard–sphere" interaction? *Phys. Rev. E*, **66**, 060501-1 (2002).
[38] B. Hancock, M. Dutt, A.C. Bentham, J. Elliott. Ordered packing induced by simultaneous shear and compaction. In *Powders and Grains 2005*, R. Garcia-Rojo, H.J. Herrmann, S McNamara (Eds.), pp. 25–28, Balkema, Rotterdam (2005).
[39] G. Gonnella, E. Orlandini, J.M. Yeomans. Spinodal decomposition to a lamellar phase: effects of hydrodynamic flow. *Phys. Rev. Lett.*, **78**, 1695 (1997).
[40] R.D. Groot, T.J. Madden. Dynamic simulation of diblock copolymer microphase separation. *J. Chem. Phys.*, **108**, 8713 (1998).
[41] R.D. Groot, T.J. Madden, J. Tildesley. On the role of hydrodynamic interactions in block copolymer microphase separation. *J. Chem. Phys.*, **110**, 9739 (1999).